NEOPLASIA
www.neoplasia.com

Volume 12 Number 12 December 2010 pp. 1023–1030 1023

Anticancer Effects of the Nitric Oxide–Modified Saquinavir Derivative Saquinavir-NO against Multidrug-Resistant Cancer Cells[1,2]

Florian Rothweiler*, Martin Michaelis*, Peter Brauer*, Jürgen Otte*, Kristoffer Weber†, Boris Fehse†, Hans Wilhelm Doerr*, Michael Wiese‡, Jörg Kreuter§, Yousef Al-Abed¶, Ferdinando Nicoletti# and Jindrich Cinatl Jr*

*Institut für Medizinische Virologie, Klinikum der J.W. Goethe-Universität, Frankfurt am Main, Germany; †Forschungsabteilung Zell- und Gentherapie, Interdisziplinäre Klinik und Poliklinik für Stammzelltransplantation, Universitätsklinikum Hamburg-Eppendorf, Hamburg, Germany; ‡Pharmaceutical Institute, University of Bonn, Bonn, Germany; §Institute for Pharmaceutical Technology, Biocenter Johann Wolfgang Goethe-University, Frankfurt (Main), Germany; ¶Feinsten Institute for Medical Research, Laboratory of Medicinal Chemistry, North Shore Long Island Jewish Health System, Manhasset, NY, USA; #Department of Biomedical Sciences, University of Catania, Catania, Italy

Abstract

The human immunodeficiency virus (HIV) protease inhibitor saquinavir shows anticancer activity. Although its nitric oxide–modified derivative saquinavir-NO (saq-NO) was less toxic to normal cells, it exerted stronger inhibition of B16 melanoma growth in syngeneic C57BL/6 mice than saquinavir did. Saq-NO has been shown to block proliferation, up-regulate p53 expression, and promote differentiation of C6 glioma and B16 cells. The anticancer activity of substances is frequently hampered by cancer cell chemoresistance mechanisms. Therefore, we here investigated the roles of p53 and the ATP-binding cassette (ABC) transporters P-glycoprotein (P-gp), multidrug resistance–associated protein 1 (MRP1), and breast cancer resistance protein 1 (BCRP1) in cancer cell sensitivity to saq-NO to get more information about the potential of saq-NO as anticancer drug. Saq-NO exerted anticancer effects in lower concentrations than saquinavir in a panel of human cancer cell lines. Neither p53 mutation or depletion nor expression of P-gp, MRP1, or BCRP1 affected anticancer activity of saq-NO or saquinavir. Moreover, saq-NO sensitized P-gp–, MRP1-, or BCRP1-expressing cancer cells to chemotherapy. Saq-NO induced enhanced sensitization of P-gp– or MRP1-expressing cancer cells to chemotherapy compared with saquinavir, whereas both substances similarly sensitized BCRP1-expressing cells. Washout kinetics and ABC transporter ATPase activities demonstrated that saq-NO is a substrate of P-gp as well as of MRP1. These data support the further investigation of saq-NO as an anticancer drug, especially in multidrug-resistant tumors.

Neoplasia (2010) 12, 1023–1030

Introduction

Anti–human immunodeficiency virus (HIV) drugs have been considered as potential anticancer drugs since the early 1990s [1]. The HIV protease inhibitors were developed in the early 1990s and were subsequently included in highly active antiretroviral therapy treatment regimens. The idea that HIV protease inhibitors may also exert direct anticancer effects stems from the observation that successful treatment of HIV-related Kaposi sarcoma by highly active antiretroviral

Address all correspondence to: Prof. Dr. Jindrich Cinatl, Jr, Institut für Medizinische Virologie, Klinikum der J.W. Goethe-Universität, Paul Ehrlich-Str. 40, 60596 Frankfurt am Main, Germany. E-mail: Cinatl@em.uni-frankfurt.de

[1]The authors thank the friendly society "Hilfe für krebskranke Kinder Frankfurt e.V." and its foundation "Frankfurter Stiftung für krebskranke Kinder" for support.

[2]This article refers to supplementary materials, which are designated by Figures W1 to W3 and are available online at www.neoplasia.com.

Received 17 June 2010; Revised 27 August 2010; Accepted 31 August 2010

 1522-8002/10/$25.00
DOI 10.1593/neo.10856

therapy was not always directly connected with immune reconstitution [2,3]. In the meantime, different antitumor mechanisms have been described for HIV protease inhibitors [1].

Saquinavir was the first US Food and Drug Administration–approved HIV protease inhibitor [1]. The substance exerts non–immune-mediated anticancer activity by mechanisms including inhibition of angiogenesis through inhibition of proteolysis of matrix metalloprotease 2, inhibition of proteasome activity, inhibition of nuclear factor κB, and inhibition of Akt phosphorylation [4–9]. In cells from different cancer entities, saquinavir induced apoptosis in a concentration-dependent manner and increased the radiosensitivity of prostate cancer cells [5]. Moreover, saquinavir was more effective in imatinib-resistant chronic myelogenous leukemia cell line than in an imatinib-sensitive one and in sensitized imatinib-resistant myelogenous leukemia cells to imatinib [10].

ATP-binding cassette (ABC) transporters are ATP-dependent pumps that transport substances across biologic membranes. They play important roles in general in the passage of drugs through cellular and tissue barriers and in cancer cell chemoresistance phenotypes [11–14]. Saquinavir has been described to be a substrate of P-glycoprotein (*P-gp*, also called multidrug resistance gene 1 [*MDR1*], the gene product of *ABCB1*), and the multidrug resistance proteins 1 and 2 (MRP1 and MRP2) [15–19]. Moreover, saquinavir was shown to be an inhibitor of the breast cancer resistance protein (BCRP1, gene product of *ABCG2*) but not a substrate [20,21].

Recently, a nitric oxide–modified derivative, saquinavir-NO (saq-NO), was synthesized and investigated for anticancer activity [22]. In contrast to saquinavir, saq-NO had no effect on the viability of primary cells, and it drastically reduced B16 mouse melanoma growth in syngeneic C57BL/6 mice. At the equivalent of the 100% lethal dose of saquinavir, saq-NO treatment caused no apparent signs of toxicity. Saq-NO blocked the proliferation of C6 rat glioma and B16 cells, upregulated p53 expression, and promoted the differentiation of these two cell types into oligodendrocytes or Schwann-like cells, respectively. Although saquinavir has been supposed to decrease tumor cell viability by inhibiting Akt, saq-NO did not exert its anticancer effects by inhibition of the phosphatidylinositol 3-kinase/Akt signaling pathway [22].

To gain further insights in the antitumoral potential of saq-NO, we compared the efficacies of saquinavir and saq-NO in the context of prominent cancer cell chemoresistance mechanisms. The effects of saquinavir or saq-NO were studied in cell lines expressing the ABC transporters P-gp, MRP1, or BCRP1. Moreover, the influence of both substances on ABC transporter–mediated cellular drug efflux was examined. In addition, Saq-NO was suggested to act (in part) through activation of p53 [22]. P53 is known to be frequently inactivated in cancer cells, and loss of p53 function contributes to cancer cell chemoresistance [23]. Therefore, we also compared anticancer effects of saquinavir and saq-NO in cancer cells in dependence of p53 function.

Materials and Methods

Cell Lines

The neuroblastoma cell line UKF-NB-3 as well as the UKF-NB-3 subline adapted to 10 ng/ml vincristine (UKF-NB-3^{r}VCR^{10}) were established as described before [24]. The alveolar rhabdomyosarcoma cell line Rh30 was kindly provided by Dr P.J. Houghton (St Jude's Children's Research Hospital, Memphis, TN). The vincristine-resistant rhabdomyosarcoma cell line Rh30^{r}VCR^{10} was established by adaptation of Rh30 cells to growth in the presence of vincristine 10 ng/ml [25]. P53-negative and P-gp–negative PC-3 prostate cancer cells expressing low MRP1 levels were received from ATCC (Manassas, VA). The vincristine-resistant subline PC-3^{r}VCR^{20} was established by adaptation of PC-3 to growth in the presence of vincristine 20 ng/ml resulting in a cell line showing high MRP1 overexpression but no P-gp expression [25].

P53 status, P-gp expression, MRP1 expression, and BCRP1 expression of the investigated cell lines are shown in Table 1 [24–26] (own unpublished data). All cell lines were propagated in Iscove's modified Dulbecco medium supplemented with 10% FBS, 100 IU/ml penicillin, and 100 mg/ml streptomycin at 37°C.

Viral Transduction

Standard molecular cloning techniques were used to generate lentiviral vectors based on Lentiviral Gene Ontology (LeGO) vector technology [27] (www.lentigo-vectors.de). To suppress expression of p53, short hairpin RNA (shRNA) against p53 was used (at least 70% downregulation; Figure W1). For overexpression of ABC transporters, complementary DNA (cDNA) coding for P-gp (approximately 50-fold increased expression; Figure W2) and for BCRP1 (approximately 400-fold increased expression; Figure W3) was used.

Drugs

Vincristine, verapamil, NEM (*N*-ethylmaleimide), and GS (reduced glutathione) were obtained from Sigma-Aldrich (Deisenhofen, Germany). Rhodamine 123 (R123) was purchased from Merck Biosciences (Darmstadt, Germany). Saquinavir was obtained from Roche (Grenzach-Wyhlen, Germany). Mitoxantron was received from GRY Pharma (Kirchzarten, Germany). MK571 and 5-carboxyfluorescein diacetate (5-CFDA) were obtained from Calbiochem (through Merck KGaA, Darmstadt, Germany). Saq-NO and WK-X-34 were synthesized as described before [22,28].

Viability Assay

Cell viability was tested by the 3-(4,5-dimethylthiazol-2-yl)-2,5-diphenyltetrazolium bromide (MTT) dye reduction assay after 96 hours of incubation, modified as described before [29]. All experiments were performed at least in triplicate.

Flow Cytometry and Investigation of Efflux of ABC Transporter Substrates

Antibodies directed against P-gp (Alexis Biochemicals through AXXORA Deutschland, Lörrach, Germany), MRP1, and breast cancer resistance protein (BCRP1/ABCG2; both Kamiya Biomedical Company, Seattle, WA) followed by secondary antibody labeled with phycoerythrin (PE; R&D, Wiesbaden, Germany) were used to detect protein expression by flow cytometry (FACSCalibur; BD Biosciences, Heidelberg, Germany).

To investigate P-gp–mediated substance efflux, cells were preincubated with different concentrations of saquinavir and saq-NO for 30 minutes. Verapamil 10 μM was used as a positive control for P-gp–mediated efflux. R123 1 μM was added for another 30 minutes. Then, the cell culture medium was removed, cells were washed three times with PBS, and fresh medium containing verapamil, saquinavir, or saq-NO was added. After another 45 minutes, cellular fluorescence was analyzed by flow cytometry (FACSCalibur). R123 was detected at the FL1 channel.

Table 1. Cellular p53 Status, P-gp Expression, MRP1 Expression, BCRP1 Expression, and Tumor Cell Sensitivity to Saquinavir and Saq-NO.

Cell Line	p53 Status*	P-gp†	MRP1‡	BCRP1§	Saquinavir IC_{50} (μM)	Saq-NO IC_{50} (μM)
UKF-NB-3	WT	–	–	–	23.2 ± 6.7	9.40 ± 2.0¶
UKF-NB-3^{r}VCR^{10}	mut (C135F)	+	–	–	18.9 ± 4.5	6.6 ± 1.5¶
UKF-NB-3^{MDR1}	WT	+	–	–	27.8 ± 5.3	13.5 ± 2.3¶
UKF-NB-3$^{LeGO\text{-}Cer2\#}$	WT	–	–	–	21.0 ± 1.4	10.3 ± 2.4¶
UKF-NB-3^{BCRP1}	WT	–	–	+	27.5 ± 5.0	11.5 ± 1.2¶
UKF-NB-3$^{LeGO\text{-}iG2**}$	WT	–	–	–	20.4 ± 3.6	10.1 ± 0.9¶
UKF-NB-3$^{p53\text{-}shRNA}$	depl.	–	–	–	20.2 ± 4.3	9.7 ± 1.3¶
UKF-NB-3$^{scr\text{-}shRNA††}$	WT	–	–	–	21.3 ± 2.1	9.3 ± 1.7¶
Rh30	mut (R273C)	–	–	–	18.7 ± 3.0	8.4 ± 3.8¶
Rh30^{r}VCR^{10}	mut (R273C)	+	–	–	26.7 ± 3.5	12.7 ± 1.9¶
PC-3	del.	–	–	–	14.3 ± 2.0	5.6 ± 0.7¶
PC-3^{r}VCR^{20}	del.	–	+	–	16.1 ± 1.9	7.5 ± 0.8¶

Values are mean ± SD from three independent experiments.
*p53 status: WT = wild-type p53, mut = mutated p53, depl. = shRNA-induced p53 depletion, del. = deleted.
†P-gp expression: + = overexpression, – = no overexpression.
‡MRP1 expression: + = overexpression, – = no overexpression.
§BCRP1 expression: + = overexpression, – = no overexpression.
¶$P < .05$ relative to saquinavir.
#Control vector for MDR1 expressing only Cerulean.
**Control vector for BCRP1 expressing only eGFP.
††Control vector for p53-shRNA expressing scrambled shRNA.

To investigate MRP1-mediated efflux, the same protocol as for P-gp–mediated efflux was carried out with MRP1-expressing cell line PC-3^{r}VCR^{20}, using the MRP1-substrate 5-CFDA and the MRP1 inhibitor MK571 as a positive control. 5-CFDA was detected at the FL1 channel.

For washout kinetic experiments, cells were incubated for 1 hour with 1 μM R123 (P-gp substrate) or with 4 μM 5-CFDA (MRP1 substrate), respectively. Saquinavir 20 μM, saq-NO 20 μM, verapamil 10 μM (positive control for P-gp), or MK571 10 μM (positive control for MRP1) was added immediately. Cells were resuspended in supplemented medium, and cellular fluorescence was measured after different time points (t_0, t_5, t_{15}, t_{30}, t_{60}, and t_{120} minutes) by flow cytometry (FACSCalibur).

To determine IC_{50} values for P-gp–mediated drug efflux, P-gp–expressing cells were incubated for 1 hour with 1 μM R123. Then, cell culture medium was removed, cells were washed three times with PBS, fresh medium (with or without saquinavir or saq-NO) was added, and cellular fluorescence was measured immediately (t_0) and after 15 minutes (t_{15}). Then, t_{15} was subtracted from t_0. R123 efflux ($t_0 - t_{15}$) in the absence of drugs was defined as 100% efflux. The R123 efflux ($t_0 - t_{15}$) in the presence of saquinavir or saq-NO was expressed in percent relative to R123 efflux ($t_0 - t_{15}$) in the absence of drugs. The concentrations that inhibit 50% of P-gp–mediated drug efflux were calculated and expressed as IC_{50} values.

All experiments were performed at least in triplicate.

Determination of ATPase Activity

The P-gp–ATPase activity and the MRP1-ATPase activity were determined using membrane preparations (Pgp-Membran: BD Bio sciences; MRP1-membrane: Solvo Biotechnology, Budapest, Hungary) and an established kit (BD Biosciences) following the manufacturer's instruction. All experiments were performed at least in triplicate.

Western Blot

Cells were lysed in Triton X sample buffer and separated by SDS-PAGE, as described before [30]. Proteins were detected using specific antibodies against β-actin (Sigma, Munich, Germany) or p53 (Alexis Biochemicals through AXXORA Deutschland) and were visualized by enhanced chemiluminescence using a commercially available kit (Amersham through GE Healthcare, Munich, Germany). All experiments were performed at least in triplicate.

Fluorescence Microscopy

Pictures were taken with an IX71 fluorescence microscope (Olympus, Hamburg, Germany). Cerulean was detected at 433/475 nm (excitation/emission), enhanced green fluorescent protein was detected at 484/507 nm (excitation/emission), and mCherry was detected at 587/610 nm (excitation/emission).

Statistical Analysis

Two groups were compared by *t*-test. More groups were compared by ANOVA with subsequent Student-Newman-Keuls test.

Results

Influence of Saquinavir and Saq-NO on Cancer Cell Viability

Saq-NO caused a stronger decrease in cancer cell viability than saquinavir in all investigated cell lines (Table 1). P-gp expression, BCRP1 expression, or p53 status (wild-type, mutated, loss of expression) did not significantly influence cancer cell sensitivity to both substances.

To further investigate the role of p53 and p53 wild-type cell line UKF-NB-3 was transduced with LeGO vectors [27] containing shRNA against p53 to suppress p53 expression (UKF-NB-3$^{p53\text{-}shRNA}$; Figure W1). UKF-NB-3$^{p53\text{-}shRNA}$ cells and the cell line resulting from transduction of UKF-NB-3 with control (scrambled) shRNA (UKF-NB-3$^{scr\text{-}shRNA}$; Figure W1) showed no differences in IC_{50} values for saquinavir and saq-NO, when compared with UKF-NB-3 (Table 1). Therefore, the saquinavir- and saq-NO–induced decreases in cancer cell viability do not depend on p53 activity.

Influence of Saquinavir and Saq-NO on P-gp Function

Saquinavir was already shown to interfere with the P-gp–mediated drug efflux [15,16,19]. Here, we compared the effects of saquinavir

and saq-NO on P-gp. First, the influence of both drugs was investigated on sensitivity of the P-gp–expressing cell lines to the structurally different P-gp substrates vincristine, actinomycin D, and paclitaxel (Table 2). Nontoxic saq-NO concentrations caused stronger (4- to 80-fold) sensitization of UKF-NB-3^{r}VCR^{10} cells and Rh30^{r}VCR^{10} cells to all three chemotherapeutic drugs than saquinavir. The effects of vincristine, actinomycin D, or paclitaxel on the parental cell lines UKF-NB-3 and Rh30 that do not express P-gp were not affected by nontoxic concentrations of saquinavir or saq-NO.

To further investigate the influence of saquinavir and saq-NO on P-gp (MDR1), UKF-NB-3 cells were transduced with LeGO vectors [27] containing cDNA coding for MDR1 to induce overexpression of P-gp (UKF-NB-3^{MDR1}; Figure W2). UKF-NB-3^{MDR1} cells and the cell line resulting from transduction of UKF-NB-3 with empty control vector LeGO-Cer2 (UKF-NB-3$^{LeGO\text{-}Cer2}$; Figure W2) displayed similar sensitivity to saquinavir and saq-NO as UKF-NB-3 (Table 1).

Effects of different saquinavir and saq-NO concentrations were investigated for their influence on vincristine sensitivity of UKF-NB-3^{MDR1} cells (Table 3). Saquinavir and saq-NO both sensitized UKF-NB-3^{MDR1} cells to vincristine in a concentration-dependent manner, whereas saq-NO again exerted considerably stronger effects (up to 30-fold).

R123 (rhodamine 123) is a fluorescent dye that is transported by P-gp. Flow cytometry analysis indicated that saquinavir and saq-NO increased R123 fluorescence in UKF-NB-3^{r}VCR^{10} and UKF-NB-3^{MDR1} cells (Figure 1*A*) with saq-NO showing higher potency than saquinavir. The concentrations that inhibited R123 efflux by 50% (IC_{50}) were for saquinavir 9.39 ± 2.81 μM in UKF-NB-3^{r}VCR^{10} cells and 2.45 ± 0.33 μM in UKF-NB-3^{MDR1} cells. The IC_{50} values for saq-NO were 0.70 ± 0.14 μM in UKF-NB-3^{r}VCR^{10} cells and 0.053 ± 0.021 μM in UKF-NB-3^{MDR1} cells.

To examine whether saq-NO may be a P-gp substrate, two experiments were performed. Washout kinetics were determined, that is, UKF-NB-3^{r}VCR^{10} and UKF-NB-3^{MDR1} cells were incubated with R123 in the presence or absence of saq-NO, saquinavir, or verapamil (a known P-gp substrate). Then, cells were washed, and cellular fluorescence was regularly measured by flow cytometry. Rapid decrease of R123 fluorescence indicated that saq-NO and saquinavir are transported by P-gp (Figure 1*B*). Moreover, the influence of saquinavir and saq-NO on P-gp–ATPase activity was measured. Saq-NO and saq stimulated P-gp–ATPase activity, further confirming that saq-NO and saquinavir are both P-gp substrates (Figure 1*C*).

Table 3. Sensitization of Stably P-gp–expressing MDR1-Transduced Cells (UKF-NB-3^{MDR1}) to Vincristine by Saq, Saq-NO, or Verapamil.

	IC_{50}* Vincristine (ng/ml)	Fold Sensitization†
Vincristine	13.17 ± 1.35	
Vincristine + verapamil 10 μM	0.07 ± 0.004‡	188.1
Vincristine + saq 10 μM	3.21 ± 0.71‡	4.10
Vincristine + saq 5 μM	6.66 ± 1.72‡	2.0
Vincristine + saq 2.5 μM	9.41 ± 2.22	1.4
Vincristine + saq-NO 10 μM	0.11 ± 0.01‡,§	119.7
Vincristine + saq-NO 5 μM	0.85 ± 0.15‡,§	15.5
Vincristine + saq-NO 2.5 μM	3.35 ± 0.93‡,§	3.9

Values are mean ± SD from three independent experiments.
*Concentration that decreases cell viability by 50%.
†IC_{50} vincristine/IC_{50} vincristine + saq, saq-NO, or verapamil.
‡$P < .05$ relative to vincristine alone.
§$P < .05$ relative to vincristine + corresponding saq concentration.

Influence of Saquinavir and Saq-NO on MRP1 Function

Saquinavir was shown to interfere with MRP1-mediated drug efflux as a substrate [17,18]. In concordance, saquinavir enhanced sensitivity of MRP1-expressing PC-3^{r}VCR^{20} to the MRP1 substrate vincristine (Table 4). Moreover, saquinavir increased accumulation of the fluorescent dye 5-CFDA known to be a MRP1 substrate (Figure 2*A*). Washout kinetics revealed a rapid decline of 5-CFDA fluorescence in the presence of saquinavir (Figure 2*B*), and determination of MRP1-ATPase activity showed that saquinavir stimulated MRP1 activity (Figure 2*C*) confirming that saquinavir is a MRP1 substrate. In comparison to saquinavir, Saq-NO induced enhanced sensitization of PC-3^{r}VCR^{20} cells to vincristine (Table 4) and increased 5-CFDA accumulation in PC-3^{r}VCR^{20} cells (Figure 2*A*). Washout kinetics (Figure 2*B*) and measurement of MRP1-ATPase activity (Figure 2*C*) demonstrated that Saq-NO is like saquinavir a MRP1 substrate.

Table 2. Sensitization of Cancer Cells to Structurally Different Anticancer Drugs Known to Be P-gp Substrates by Saq or Saq-NO Concentrations That Did Not Affect Cancer Cell Viability.

Cell Line (P-gp Status*)	Anticancer Drug	IC_{50}† (ng/ml) Anticancer Drug	Saq (μM)	IC_{50} (ng/ml) Anticancer Drug in the Presence of Saq (Fold Sensitization‡)	Saq-NO (μM)	IC_{50} (ng/ml) Anticancer Drug in the Presence of Saq-NO (Fold Sensitization§)
UKF-NB-3 (–)	Vincristine	0.20 ± 0.08	10	0.14 ± 0.02 (1.4)	5	0.10 ± 0.04 (2.0)
	Actinomycin D	0.19 ± 0.07	10	0.18 ± 0.06 (1.1)	5	0.16 ± 0.05 (1.2)
	Paclitaxel	1.12 ± 0.35	10	0.79 ± 0.15 (1.4)	5	0.88 ± 0.20 (1.3)
UKF-NB-3^{r}VCR^{10} (+)	Vincristine	40.29 ± 5.07	10	3.43 ± 0.93¶ (11.8)	5	0.31 ± 0.04¶,# (130.0)
	Actinomycin D	6.58 ± 1.43	10	3.18 ± 1.15¶ (2.1)	5	0.22 ± 0.02¶,# (29.9)
	Paclitaxel	40.86 ± 7.48	10	12.26 ± 2.23¶ (3.3)	5	3.05 ± 0.34¶,# (13.4)
Rh30 (–)	Vincristine	0.56 ± 0.15	10	0.32 ± 0.07 (1.8)	2.5	0.39 ± 0.13 (1.4)
	Actinomycin D	0.32 ± 0.10	10	0.28 ± 0.03 (1.1)	2.5	0.23 ± 0.07 (1.4)
	Paclitaxel	4.48 ± 0.51	10	3.62 ± 0.65 (1.2)	2.5	3.73 ± 0.64 (1.2)
Rh30^{r}VCR^{10} (+)	Vincristine	37.21 ± 6.89	10	17.36 ± 3.41¶ (2.1)	5	0.21 ± 0.09¶,# (177.2)
	Actinomycin D	12.85 ± 2.75	10	4.81 ± 1.39¶ (2.7)	5	1.49 ± 0.17¶,# (8.6)
	Paclitaxel	90.74 ± 10.91	10	36.93 ± 7.18¶ (2.5)	5	6.77 ± 1.19¶,# (13.4)

Values are mean ± SD from three independent experiments.
*+ = high P-gp expression, – = low P-gp expression.
†Concentration that decreases cell viability by 50%.
‡IC_{50} anticancer drug/IC_{50} anticancer drug + saq.
§IC_{50} anticancer drug/IC_{50} anticancer drug + saq-NO.
¶$P < .05$ relative to anticancer drug alone.
#$P < .05$ relative to anticancer drug + saq.

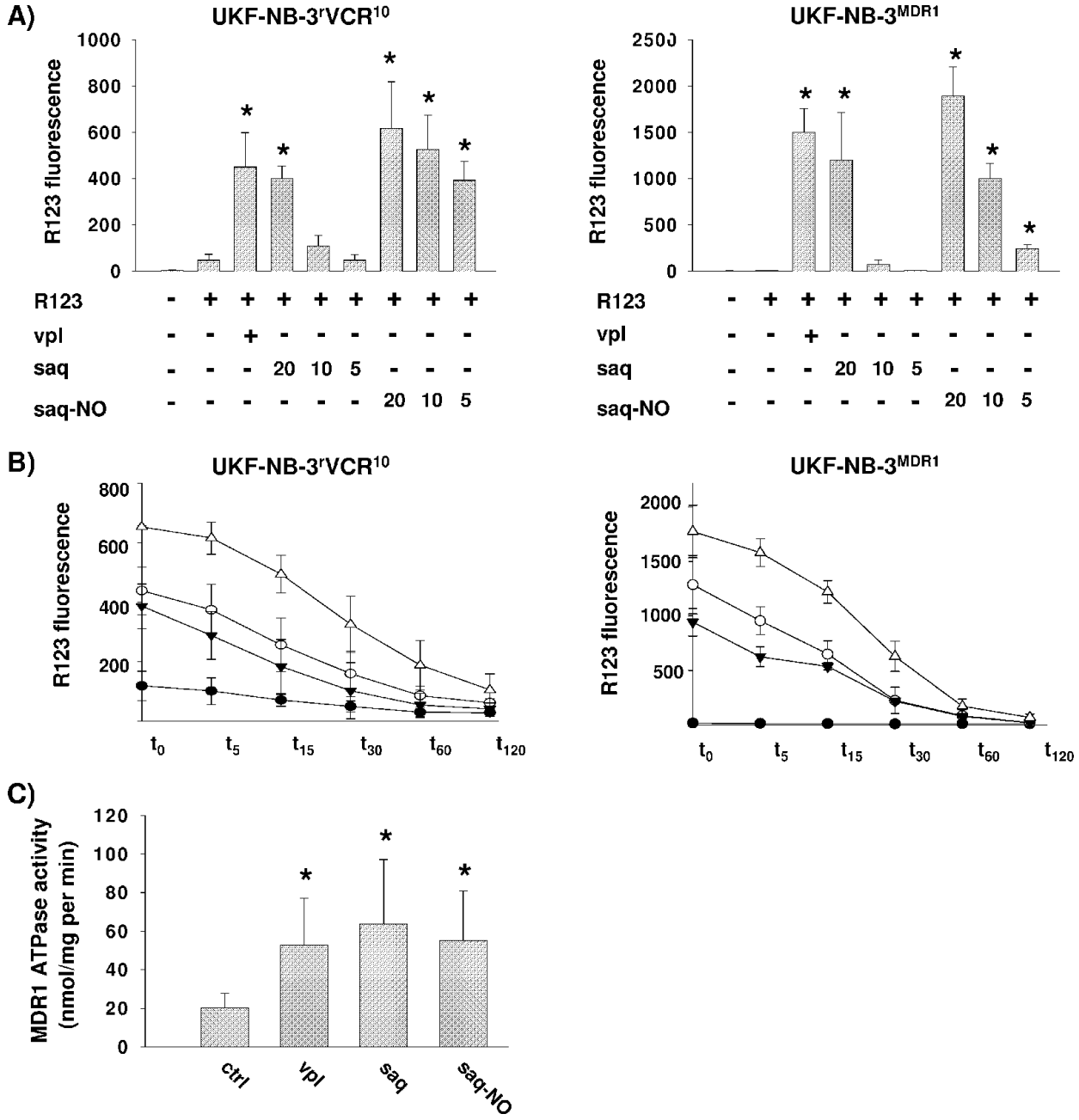

Figure 1. Influence of saquinavir and saq-NO on P-gp activity. (A) Flow cytometric analysis of R123 accumulation in the P-gp–expressing cell lines UKF-NB-3rVCR^{10} and UKF-NB-3^{MDR1}. Cells were incubated with 1 μM R123. Verapamil 10 μM (vpl) was used as a positive control. Saquinavir (saq) and saq-NO were tested at concentrations of 20, 10, and 5 μM, respectively. *$P < .05$ compared with R123. (B) Flow cytometric analysis of washout kinetics for R123 in UKF-NB-3rVCR^{10} or UKF-NB-3^{MDR1} cells. Cells were incubated with 1 μM R123 for 1 hour, together with 10 μM verapamil (positive control), 10 μM saquinavir, or 10 μM saquinavir-NO. R123 specific fluorescence was measured at FL1 channel after different time points (t_0, t_5, t_{15}, t_{30}, t_{60}, and t_{120} minutes): (–●–) 1 μM R123, (–○–) 10 μM verapamil, (–▼–) 10 μM saquinavir, (–▵–) 10 μM saq-NO. (C) P-gp–ATPase activity after incubation with 10 μM verapamil (vpl; positive control), 10 μM saquinavir (saq), or 10 μM saq-NO. *$P < .05$ compared with untreated control (ctrl). All data represent mean ± SD from three independent experiments.

Influence of Saquinavir and Saq-NO on BCRP1 Function

Saquinavir was shown to be an inhibitor of BCRP1 but not a substrate [20,21]. To investigate the influence of saquinavir and saq-NO on BCRP1 function, UKF-NB-3 cells were transduced with LeGO vectors [27] containing cDNA coding for BCRP1 to induce overexpression of BCRP1 (UKF-NB-3^{BCRP1}; Figure W3). UKF-NB-3^{BCRP1} cells and the cell line resulting from transduction of UKF-NB-3 with empty control vector LeGO-iG2 (UKF-NB-3$^{LeGO\text{-}iG2}$; Figure W3) showed similar sensitivity to saquinavir and saq-NO as UKF-NB-3 (Table 1).

Investigations in UKF-NB-3^{BCRP1} cells revealed that saquinavir and saq-NO sensitized BCRP1-expressing cells to the BCRP1 substrate mitoxantron in a similar manner (Table 5). Compared with the BCRP1 inhibitor WK-X-34 [28] as well as the effects of saq-NO

Table 4. Sensitization of MRP1-Expressing PC-3^{r}VCR^{20} Cells to Vincristine by Saq, Saq-NO, or MK571 (MRP1 Inhibitor).

	IC_{50}* Vincristine	Fold Sensitization†
Vincristine	33.10 ± 4.07	
Vincristine + MK571 10 μM	12.54 ± 1.88‡	3.7
Vincristine + saq 5 μM	4.28 ± 0.61‡	7.7
Vincristine + saq 2.5 μM	8.76 ± 1.19‡	3.8
Vincristine + saq-NO 5 μM	2.73 ± 0.42‡,§	12.1
Vincristine + saq-NO 2.5 μM	4.51 ± 0.73‡,§	7.3

Values are mean ± SD from three independent experiments.
*Concentration that decreases cell viability by 50%.
$^\dagger IC_{50}$ vincristine/IC_{50} vincristine + saq, saq-NO, or MK571.
$^\ddagger P < .05$ relative to vincristine alone.
$^\S P < .05$ relative to vincristine + corresponding saq concentration.

on P-gp, effects were moderate. Therefore, effects of saq-NO on BCRP1 are not superior to those exerted by saquinavir.

Discussion

HIV protease inhibitors including saquinavir exert anticancer activities [1]. Recently, saq-NO, a nitric oxide–modified derivative of saquinavir was synthesized, exerting stronger antitumoral effects but lower toxic adverse effects [22]. Here, we compared the effects of saquinavir and saq-NO on human cancer cells in dependence of cellular p53 status, P-gp expression, MRP1 expression, and BCRP1 expression.

The anticancer effects of saq-NO were paralleled by activation of p53 [22], and p53 activation had been documented to be involved in the anticancer activity of the HIV protease inhibitor nelfinavir [31]. However, HIV protease inhibitors including saquinavir were found to also target cells with nonfunctional p53 [1,5]. In our experiments, saq-NO and saquinavir exerted similar toxic effects against p53 wild-type, p53-mutated, and p53-deleted cancer cells, with saq-NO being the approximately three-fold more effective substance. In addition, knock down of the *p53* gene in the p53 wild-type UKF-NB-3 cell line using a lentiviral vector expressing shRNA directed against p53 did not influence UKF-NB-3 cell sensitivity to saq-NO or saquinavir. Therefore, the anticancer activity of saq-NO includes cancer cells with p53 mutations or deletions. These findings are important because p53 is the gene most frequently found mutated in cancer cells and that loss of p53 function contributes to cancer cell chemoresistance [32].

Also, the expression of the ABC transporters P-gp, MRP1, or BCRP1 did not affect cancer cell sensitivity to saquinavir or saq-NO. Because the expression of these transporters has been associated with cancer cell multidrug resistance [11–14], this finding favors the use of saq-NO for the treatment of drug-resistant cancer cells. Moreover, ABC transporters including P-gp, MRP1, and BCRP1 have been suggested to be expressed on so-called "cancer stem cells" or "tumor-initiating cells" that are regarded to be critical targets in anticancer therapy at least in some cancer entities [33–35].

In addition to the direct anticancer effects of saq-NO in ABC transporter–expressing cancer cells, we investigated the effects of saq-NO on P-gp–, MRP1-, and BCRP1-mediated drug efflux. Substances that interfere with ABC transporter function can sensitize ABC transporter–expressing cancer cells to cytotoxic drugs. HIV protease inhibitors including saquinavir have already been shown to affect ABC transporter–mediated drug efflux [15–21]. Saq-NO interfered substantially stronger with the P-gp–mediated drug efflux than saquinavir. As indicated by washout kinetics and P-gp–ATPase activity, saq-NO is like saquinavir, a P-gp substrate that competes with other substrates for binding to P-gp. Saq-NO also exerted stronger effects on MRP1 than saquinavir, and it is like saquinavir, an MRP1

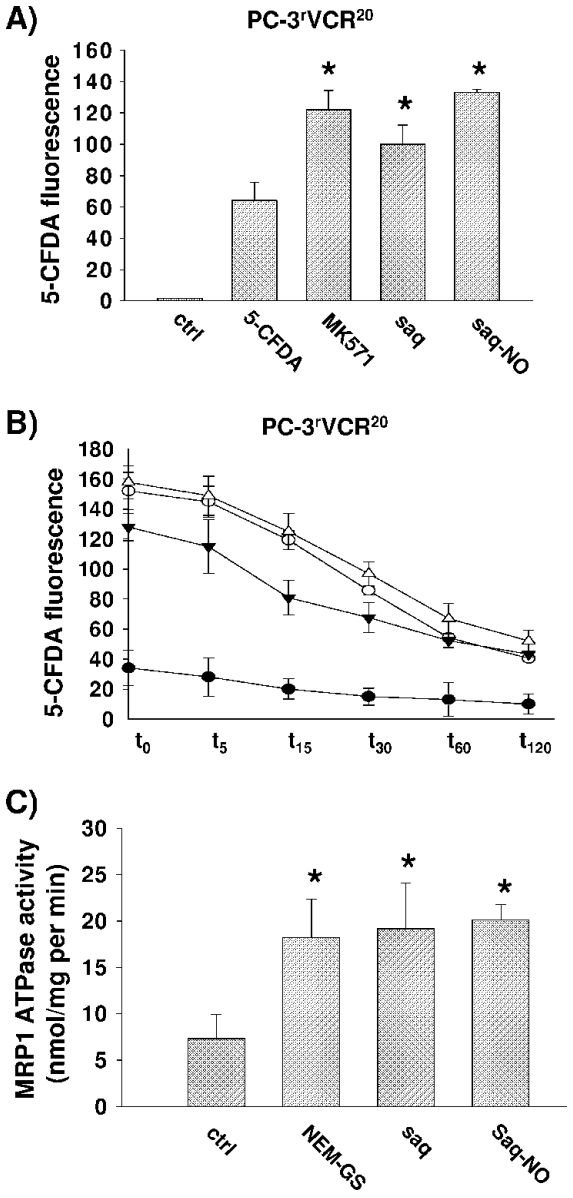

Figure 2. Influence of saquinavir and saq-NO on MRP1 activity. (A) Flow cytometric analysis of 5-CFDA accumulation in the MRP1-expressing cell line PC-3^{r}VCR^{20}. Cells were incubated with 4 μM 5-CFDA. MK571 10 μM was used as a positive control. Saquinavir (saq) and saq-NO were tested at concentrations of 10 μM. *$P < .05$ compared with 5-CFDA. (B) Flow cytometric analysis of washout kinetics for 5-CFDA in PC-3^{r}VCR^{20} cells. Cells were incubated with 4 μM 5-CFDA for 1 hour, together with 10 μM MK571 as a positive control, 10 μM saquinavir (saq), or 10 μM saquinavir-NO (saq-NO). 5-CFDA–specific fluorescence was measured at FL1 channel after different time points (t_0, t_5, t_{15}, t_{30}, t_{60}, and t_{120} minutes): (–●–) 4 μM 5-CFDA, (–○–) 10 μM MK571, (–▼–) 10 μM saquinavir, (–△–) 10 μM saquinavir-NO. (C) MRP1-ATPase activity after incubation with 10 μM NEM-GS (*N*-ethylmaleimide glutathione; positive control), 10 μM saquinavir (saq), or 10 μM saquinavir-NO (saq-NO). *$P <$ .05 compared with untreated control (ctrl). All data represent mean ± SD from three independent experiments.

Table 5. Sensitization of Stably BCRP1-Expressing BCRP1-Transduced Cells (UKF-NB-3^{BCRP1}) to Mitoxantrone by Saq, Saq-NO or WK-X-34 (BCRP1 Inhibitor) Concentrations That Did Not Affect Cancer Cell Viability.

	IC_{50}* Mitoxantrone (ng/ml)	Fold Sensitization†
Mitoxantrone	45.87 ± 7.97	
Mitoxantrone + WK-X-34 1 μM	0.17 ± 0.04‡	269.8
Mitoxantrone + saq 10 μM	12.54 ± 1.88‡	3.7
Mitoxantrone + saq 5 μM	34.77 ± 10.04	1.3
Mitoxantrone + saq 2.5 μM	39.66 ± 10.44	1.2
Mitoxantrone + saq-NO 10 μM	9.62 ± 3.24‡	4.8
Mitoxantrone + saq-NO 5 μM	19.73 ± 3.64‡	2.3
Mitoxantrone + saq-NO 2.5 μM	37.73 ± 14.21	1.2

Values are mean ± SD from three independent experiments.
*Concentration that decreases cell viability by 50%.
†IC_{50} mitoxantrone/IC_{50} mitoxantrone + saq, saq-NO, or WK-X-34.
‡$P < .05$ relative to mitoxantrone alone.

substrate. In contrast, saq-NO and saquinavir exerted similar effects on BCRP1 function.

ABC transporter inhibitors, especially P-gp inhibitors, have been intensively investigated as anticancer drugs [11–14,36,37]. The first-generation inhibitors including verapamil and cyclosporine A were drugs established for other indications than cancer that had been identified to be P-gp substrates. Their use was limited by toxic (off-target) adverse effects [11–14,36,37]. Later generations were more specific and acted as noncompetitive ABC transporter inhibitors. However, although some clinical phase 1 and 2 trials with ABC transporter inhibitors seemed to be encouraging, successful phase 3 trials are missing [11–14,36,37]. Therefore, the development of ABC transporter inhibitors for anticancer therapies is currently regarded with skepticism [37]. One reason for the clinical failure of ABC transporters may be that chemoresistant cancer (stem) cells express multiple ABC transporters and inhibition of one is not sufficient [38]. The use of the broad-spectrum ABC transporter inhibitor cyclosporine A had initially shown beneficial effects in clinical trials in patients with acute myeloid leukemia [39,40], although the use of this drug in cancer is limited by its immunosuppressive effects and by numerous further severe adverse effects including nephrotoxicity [38]. Therefore, the ability to interfere with different ABC transporters may be an advantage for a potential anticancer drug. More importantly, data about the effects of potential anticancer agents are of high relevance 1) for pharmacokinetic considerations because ABC transporters are key players in the transport of substances through physiological barriers [12] and 2) for interpretation of substance effects in combination with other anticancer agents that are ABC transporter substrates.

In conclusion, we show that the saquinavir derivative saq-NO exerts stronger antitumoral effects than saquinavir. Saq-NO is equally effective against multidrug-resistant cancer cells characterized by P-gp expression, MRP1 expression, BCRP1 expression, and/or nonfunctional p53. Moreover, saq-NO shows increased inhibition of P-gp– or MRP1-mediated drug efflux in comparison to saquinavir and similar inhibitory activity on BCRP1. In this light, further investigation of saquinavir and saq-NO as potential anticancer drugs seems worthwhile, especially in combination with chemotherapeutic agents against multidrug-resistant tumor cells. Clinical experience with saquinavir is very strong, its toxicity profile is relatively mild compared with cyclosporine A or anticancer chemotherapeutics [42], and the first experimental results suggest that saq-NO may cause less toxic adverse effects than saquinavir [22].

Acknowledgments

The shRNA against p53 and the scrambled control shRNA were kindly provided by Wolfgang Deppert and Genrich Tolstong from Heinrich-Pette-Institut, Hamburg, Germany.

References

[1] Chow WA, Jiang C, and Guan M (2009). Anti-HIV drugs for cancer therapeutics: back to the future? *Lancet Oncol* **10**, 61–71.
[2] Bower M, Fox P, Fife K, Gill J, Nelson M, and Gazzard B (1999). Highly active anti-retroviral therapy (HAART) prolongs time to treatment failure in Kaposi's sarcoma. *AIDS* **13**, 2105–2111.
[3] Lebbé C, Blum L, Pellet C, Blanchard G, Vérola O, Morel P, Danne O, and Calvo F (1998). Clinical and biological impact of antiretroviral therapy with protease inhibitors on HIV-related Kaposi's sarcoma. *AIDS* **12**, F45–F49.
[4] André P, Groettrup M, Klenerman P, de Giuli R, Booth BL Jr, Cerundolo V, Bonneville M, Jotereau F, Zinkernagel RM, and Lotteau V (1998). An inhibitor of HIV-1 protease modulates proteasome activity, antigen presentation, and T cell responses. *Proc Natl Acad Sci USA* **95**, 13120–13124.
[5] Pajonk F, Himmelsbach J, Riess K, Sommer A, and McBride WH (2002). The human immunodeficiency virus (HIV)-1 protease inhibitor saquinavir inhibits proteasome function and causes apoptosis and radiosensitization in non–HIV-associated human cancer cells. *Cancer Res* **62**, 5230–5235.
[6] Sgadari C, Barillari G, Toschi E, Carlei D, Bacigalupo I, Baccarini S, Palladino C, Leone P, Bugarini R, Malavasi L, et al. (2002). HIV protease inhibitors are potent anti-angiogenic molecules and promote regression of Kaposi sarcoma. *Nat Med* **8**, 225–232.
[7] Sgadari C, Monini P, Barillari G, and Ensoli B (2003). Use of HIV protease inhibitors to block Kaposi's sarcoma and tumour growth. *Lancet Oncol* **4**, 537–547.
[8] Monini P, Sgadari C, Toschi E, Barillari G, and Ensoli B (2004). Antitumour effects of antiretroviral therapy. *Nat Rev Cancer* **4**, 861–875.
[9] Gupta AK, Cerniglia GJ, Mick R, McKenna WG, and Muschel RJ (2006). HIV protease inhibitors block Akt signaling and radiosensitize tumor cells both *in vitro* and *in vivo*. *Cancer Res* **65**, 8256–8265.
[10] Timeus F, Crescenzio N, Ricotti E, Doria A, Bertin D, Saglio G, and Tovo PA (2006). The effects of saquinavir on imatinib-resistant chronic myelogenous leukemia cell lines. *Haematologica* **91**, 711–712.
[11] Szakács G, Paterson JK, Ludwig JA, Booth-Genthe C, and Gottesman MM (2006). Targeting multidrug resistance in cancer. *Nat Rev Drug Discov* **5**, 219–234.
[12] Szakács G, Váradi A, Ozvegy-Laczka C, and Sarkadi B (2008). The role of ABC transporters in drug absorption, distribution, metabolism, excretion and toxicity (ADME-Tox). *Drug Discov Today* **13**, 379–393.
[13] Zhou SF, Wang LL, Di YM, Xue CC, Duan W, Li CG, and Li Y (2008). Substrates and inhibitors of human multidrug resistance associated proteins and the implications in drug development. *Curr Med Chem* **15**, 1981–2039.
[14] Gatti L, Beretta GL, Cossa G, Zunino F, and Perego P (2009). ABC transporters as potential targets for modulation of drug resistance. *Mini Rev Med Chem* **9**, 1102–1112.
[15] Kim RB, Fromm MF, Wandel C, Leake B, Wood AJ, Roden DM, and Wilkinson GR (1998). The drug transporter P-glycoprotein limits oral absorption and brain entry of HIV-1 protease inhibitors. *J Clin Invest* **101**, 289–294.
[16] Lee CG, Gottesman MM, Cardarelli CO, Ramachandra M, Jeang KT, Ambudkar SV, Pastan I, and Dey S (1998). HIV-1 protease inhibitors are substrates for the MDR1 multidrug transporter. *Biochemistry* **37**, 3594–3601.
[17] Williams GC, Liu A, Knipp G, and Sinko PJ (2002). Direct evidence that saquinavir is transported by multidrug resistance–associated protein (MRP1) and canalicular multispecific organic anion transporter (MRP2). *Antimicrob Agents Chemother* **46**, 3456–3462.
[18] Dallas S, Ronaldson PT, Bendayan M, and Bendayan R (2004). Multidrug resistance protein 1–mediated transport of saquinavir by microglia. *Neuroreport* **15**, 1183–1186.
[19] Ronaldson PT, Lee G, Dallas S, and Bendayan R (2004). Involvement of P-glycoprotein in the transport of saquinavir and indinavir in rat brain microvessel endothelial and microglia cell lines. *Pharm Res* **21**, 811–818.
[20] Gupta A, Zhang Y, Unadkat JD, and Mao Q (2004). HIV protease inhibitors are inhibitors but not substrates of the human breast cancer resistance protein (BCRP1/ABCG2). *J Pharmacol Exp Ther* **310**, 334–341.
[21] Weiss J, Rose J, Storch CH, Ketabi-Kiyanvash N, Sauer A, Haefeli WE, and Efferth T (2007). Modulation of human BCRP1 (ABCG2) activity by anti-HIV drugs. *J Antimicrob Chemother* **59**, 238–245.

[22] Maksimovic-Ivanic D, Mijatovic S, Miljkovic D, Harhaji-Trajkovic L, Timotijevic G, Mojic M, Dabideen D, Cheng KF, McCubrey JA, Mangano K, et al. (2009). The antitumor properties of a nontoxic, nitric oxide–modified version of saquinavir are independent of Akt. *Mol Cancer Ther* **8**, 1169–1178.

[23] Vazquez A, Bond EE, Levine AJ, and Bond GL (2008). The genetics of the p53 pathway, apoptosis and cancer therapy. *Nat Rev Drug Discov* **7**, 979–987.

[24] Kotchetkov R, Driever PH, Cinatl J, Michaelis M, Karaskova J, Blaheta R, Squire JA, Von Deimling A, Moog J, and Cinatl J Jr (2005). Increased malignant behavior in neuroblastoma cells with acquired multi-drug resistance does not depend on P-gp expression. *Int J Oncol* **27**, 1029–1037.

[25] Michaelis M, Rothweiler F, Klassert D, von Deimling A, Weber K, Fehse B, Kammerer B, Doerr HW, and Cinatl J Jr (2009). Reversal of P-glycoprotein–mediated multidrug resistance by the murine double minute antagonist nutlin-3. *Cancer Res* **69**, 416–421.

[26] Hosoi H, Dilling MB, Shikata T, Liu LN, Shu L, Ashmun RA, Germain GS, Abraham RT, and Houghton PJ (1999). Rapamycin causes poorly reversible inhibition of mTOR and induces p53-independent apoptosis in human rhabdomyosarcoma cells. *Cancer Res* **59**, 886–894.

[27] Weber K, Bartsch U, Stocking C, and Fehse B (2008). A multicolor panel of novel lentiviral "gene ontology" (LeGO) vectors for functional gene analysis. *Mol Ther* **16**, 698–706.

[28] Jekerle V, Klinkhammer W, Scollard DA, Breitbach K, Reilly RM, Piquette-Miller M, and Wiese M (2006). *In vitro* and *in vivo* evaluation of WK-X-34, a novel inhibitor of P-glycoprotein and BCRP1, using radio imaging techniques. *Int J Cancer* **119**, 414–422.

[29] Michaelis M, Suhan T, Cinatl J, Driever PH, and Cinatl J Jr (2004). Valproic acid and interferon-α synergistically inhibit neuroblastoma cell growth *in vitro* and *in vivo*. *Int J Oncol* **25**, 1795–1799.

[30] Michaelis M, Michaelis UR, Fleming I, Suhan T, Cinatl J, Blaheta RA, Hoffmann K, Kotchetkov R, Busse R, Nau H, et al. (2004). Valproic acid inhibits angiogenesis *in vitro* and *in vivo*. *Mol Pharmacol* **65**, 520–527.

[31] Yang Y, Ikezoe T, Nishioka C, Bandobashi K, Takeuchi T, Adachi Y, Kobayashi M, Takeuchi S, Koeffler HP, and Taguchi H (2006). NFV, an HIV-1 protease inhibitor, induces growth arrest, reduced Akt signalling, apoptosis and docetaxel sensitisation in NSCLC cell lines. *Br J Cancer* **95**, 1653–1662.

[32] Levine AJ and Oren M (2009). The first 30 years of p53: growing ever more complex. *Nat Rev Cancer* **9**, 749–758.

[33] Donnenberg VS and Donnenberg AD (2005). Multiple drug resistance in cancer revisited: the cancer stem cell hypothesis. *J Clin Pharmacol* **45**, 872–877.

[34] Baguley BC (2010). Multidrug resistance in cancer. *Methods Mol Biol* **596**, 1–14.

[35] Ding XW, Wu JH, and Jiang CP (2010). ABCG2: a potential marker of stem cells and novel target in stem cell and cancer therapy. *Life Sci* **86**, 631–637.

[36] Lage H (2008). An overview of cancer multidrug resistance: a still unsolved problem. *Cell Mol Life Sci* **65**, 3145–3167.

[37] Fletcher JI, Haber M, Henderson MJ, and Norris MD (2010). ABC transporters in cancer: more than just drug efflux pumps. *Nat Rev Cancer* **10**, 147–156.

[38] Dean M, Fojo T, and Bates S (2005). Tumour stem cells and drug resistance. *Nat Rev Cancer* **5**, 275–284.

[39] List AF, Kopecky KJ, Willman CL, Head DR, Persons DL, Slovak ML, Dorr R, Karanes C, Hynes HE, Doroshow JH, et al. (2001). Benefit of cyclosporine modulation of drug resistance in patients with poor-risk acute myeloid leukemia: a Southwest Oncology Group study. *Blood* **98**, 3212–3220.

[40] Smeets M, Raymakers R, Muus P, Vierwinden G, Linssen P, Masereeuw R, and de Witte T (2001). Cyclosporin increases cellular idarubicin and idarubicinol concentrations in relapsed or refractory AML mainly due to reduced systemic clearance. *Leukemia* **15**, 80–88.

[41] Kahan BD (2009). Forty years of publication of transplantation proceedings—the second decade: the cyclosporine revolution. *Transplant Proc* **41**, 1423–1437.

[42] la Porte CJ (2009). Saquinavir, the pioneer antiretroviral protease inhibitor. *Expert Opin Drug Metab Toxicol* **5**, 1313–1322.

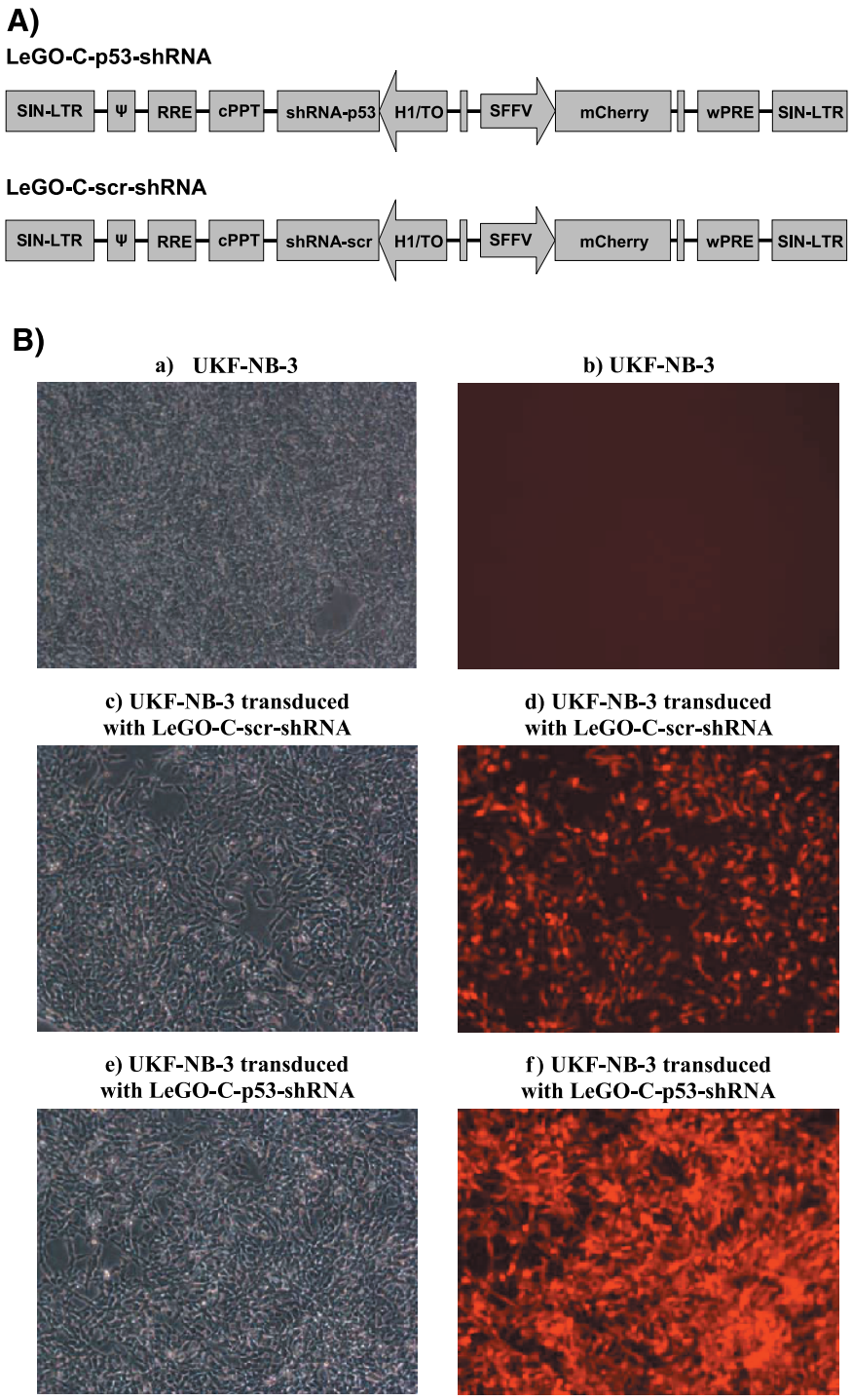

Figure W1. (A) Scheme of the lentiviral vectors, as integrated proviruses, that have been used in this study (not drawn to scale). Ψ indicates packaging signal; cPPT, central polypurine tract; H1/TO, RNA-polymerase III promoter; mCherry, a red fluorescent protein; RRE, rev-responsive element; SFFV, spleen focus–forming virus enhancer/promoter; shRNA-p53, short hairpin RNA against human p53; shRNA-scr, short hairpin RNA with no target (scrambled); SIN-LTR, self-inactivating long-terminal repeat; wPRE, Woodchuck hepatitis virus posttranscriptional regulatory element. (B) UKF-NB-3, UKF-NB-3 transduced with LeGO-C-scr-shRNA (UKF-NB-3$^{scr\text{-}shRNA}$, and UKF-NB-3 transduced with LeGO-C-p53-shRNA (UKF-NB-3$^{p53\text{-}shRNA}$) cells were photographed by inverse light microscopy (a, c, and e) and by fluorescence microscopy (b, d, and f), using an IX71 fluorescence microscope (Olympus). Fluorescence dye mCherry was detected at 587/610 nm (excitation/emission). The nontransduced control cell line UKF-NB-3 showed no fluorescence (b). In contrast, UKF-NB-3$^{scr\text{-}shRNA}$ and UKF-NB-3$^{p53\text{-}shRNA}$ cells displayed high fluorescence due to successful transduction with shRNAs (d, f). (C) Western blot was carried out with UKF-NB-3 (a), UKF-NB-3$^{p53\text{-}shRNA}$ (b), and UKF-NB-3$^{scr\text{-}shRNA}$ (c) cells, detecting p53 (Alexis Biochemicals through AXXORA Deutschland) and β-actin as control (Sigma). The cell lines UKF-NB-3 and UKF-NB-3$^{scr\text{-}shRNA}$ showed clear expression of p53 (a and c). In contrast, UKF-NB-3$^{p53\text{-}shRNA}$ cells displayed significant decreased p53-expression (b) due to successful transduction with shRNA against p53. Densitometric analysis revealed at least 70% down-regulation of p53. (D) Concentrations of the MDM2 inhibitor nutlin-3a that non-genotoxically activates p53, its enantiomer nutlin-3b that shows 150-fold lower MDM2-inhibitory activity, and of the cytotoxic drugs vincristine and doxorubicin that reduce cell viability by 50% (IC_{50}) as indicated by MTT assay. Values are mean ± SD from three independent experiments. *$P < .05$ relative to nontransfected cells.

C)

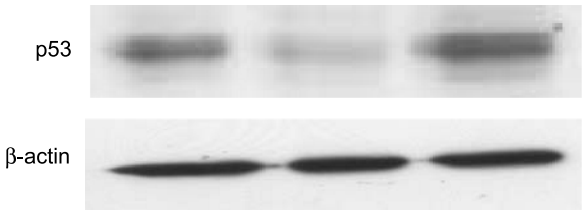

D)

Cell line	IC_{50} nutlin-3a (μM)	IC_{50} nutlin-3b (μM)	IC_{50} vincristine (ng/ml)	IC_{50} doxorubicin (ng/ml)
UKF-NB-3	0.81 ± 0.15	> 20	0.25 ± 0.06	6.22 ± 1.97
UKF-NB-3$^{p53\text{-}shRNA}$	8.23 ± 1.73*	> 20*	1.10 ± 0.21*	19.98 ± 2.61*
UKF-NB-3$^{scr\text{-}shRNA}$	0.66 ± 0.15	> 20	0.31 ± 0.05	5.94 ± 0.89

Figure W1. (*continued*).

Materials and Methods

Cloning of Lentiviral Vectors

Standard molecular cloning techniques were used to generate viral vectors based on Lentiviral Gene Ontology (LeGO) vectors [1] (also http://www.LentiGO-Vectors.de). Maps and sequence data of the vectors are available on request. The 60-bp shRNA against human p53 or the 60-bp scrambled shRNA was cloned into LeGO-C using *Xba*I and *Xho*I. The internal promoter H1/TO transcribes the shRNA against p53 or the scrambled shRNA, respectively. The internal SFFV promoter drives the expression of the red fluorescent protein mCherry as a marker gene.

Generation of Viral Particles

Cell-free viral supernatants were generated by transient transfection of 293T packaging cells as described [2], using the third-generation packaging plasmids pMDLg/pRRE and pRSV-Rev [3] together with phCMV-VSV-G [2]. Supernatants containing pseudotyped vector particles were titrated on 293T target cells. Gene transfer rates were analyzed 2 days after transduction by fluorescence-activated cell sorting (FACS). Titers of 1.5×10^7 (LeGO-C-p53-shRNA) and 2×10^7 (LeGO-C-scr-shRNA) VSV-G pseudotyped virus particles per milliliter of unconcentrated supernatants were obtained.

Cell Culture and Lentiviral Gene Transfer

All cells were cultured in their respective growth medium supplemented with penicillin/streptomycin. For transduction of UKF-NB-3 target cells, 5×10^4 cells in 500 μl of medium were plated per well in a 24-well plate. The next day, 250 μl of viral supernatant per well was added in the presence of 8 μg/ml polybrene, and the plate was centrifuged at 1000*g* for 1 hour at room temperature. After another 3 hours in the cell culture incubator, medium was replaced.

Fluorescence Microscopy

Pictures were taken using an IX71 fluorescence microscope (Olympus, Hamburg, Germany). Fluorescence dye mCherry was detected at 587 nm emission/610 nm excitation.

Western Blot

Cells were lysed in Triton X sample buffer and separated by SDS-PAGE, as described before [4]. Proteins were detected using specific antibodies against β-actin (Sigma, Munich, Germany) or p53 (Alexis Biochemicals through AXXORA Deutschland, Lörrach, Germany) and were visualized by enhanced chemiluminescence using a commercially available kit (Amersham through GE Healthcare, Munich, Germany).

MTT Assay

Cell viability was tested by the 3-(4,5-dimethylthiazol-2-yl)-2,5-diphenyltetrazolium bromide (MTT) dye reduction assay after 96 hours of incubation modified as described before [5].

References

[1] Weber K, Bartsch U, Stocking C, and Fehse B (2008). A multicolor panel of novel lentiviral "gene ontology" (LeGO) vectors for functional gene analysis. *Mol Ther* **16**, 698–706.

[2] Beyer WR, Westphal M, Ostertag W, and von Laer D (2002). Oncoretrovirus and lentivirus vectors pseudotyped with lymphocytic choriomeningitis virus glycoprotein: generation, concentration, and broad host range. *J Virol* **76**, 1488–1495.

[3] Dull T, Zufferey R, Kelly M, Mandel RJ, Nguyen M, Trono D, and Naldini L (1998). A third-generation lentivirus vector with a conditional packaging system. *J Virol* **72**, 8463–8471.

[4] Michaelis M, Michaelis UR, Fleming I, Suhan T, Cinatl J, Blaheta RA, Hoffmann K, Kotchetkov R, Busse R, Nau H, et al. (2004). Valproic acid inhibits angiogenesis *in vitro* and *in vivo*. *Mol Pharmacol* **65** (3), 520–527.

[5] Michaelis M, Suhan T, Cinatl J, Driever PH, and Cinatl J, Jr (2004). Valproic acid and interferon-α synergistically inhibit neuroblastoma cell growth *in vitro* and *in vivo*. *Int J Oncol* **25**, 1795–1799.

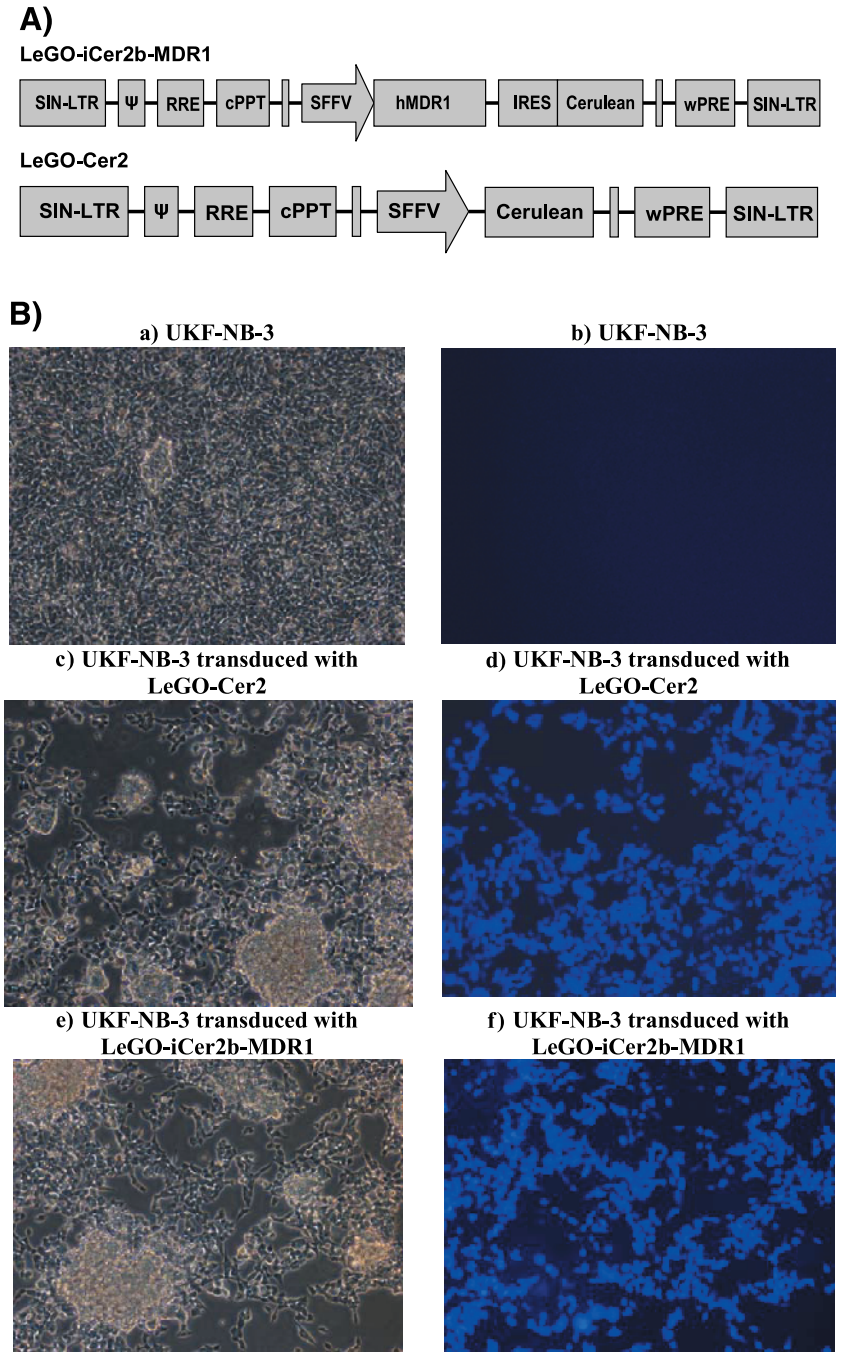

Figure W2. (A) Scheme of the lentiviral vectors, as integrated proviruses, that have been used in this study (not drawn to scale). Ψ indicates packaging signal; Cerulean, a blue variant of the enhanced green fluorescent protein; cPPT, central polypurine tract; hMDR1, human multiple drug resistance gene cDNA; IRES, internal ribosome entry site of the EMCV; RRE, rev-responsive element; SFFV, spleen focus–forming virus enhancer/promoter; SIN-LTR, self-inactivating long terminal repeat; wPRE, Woodchuck hepatitis virus posttranscriptional regulatory element. (B) UKF-NB-3, UKF-NB-3 transduced with LeGO-Cer2 (UKF-NB-$3^{LeGO\text{-}Cer2}$), and UKF-NB-3 transduced with LeGO-iCer2-MDR1 (UKF-NB-3^{MDR1}) cells were photographed by inverse light microscopy (a, c, e) and by fluorescence microscopy (b, d, f), using an IX71 fluorescence microscope (Olympus). Fluorescence dye Cerulean was detected at 433/475 nm (excitation/emission). The nontransduced control cell line UKF-NB-3 showed no fluorescence (b). In contrast, UKF-NB-$3^{LeGO\text{-}Cer2}$ and UKF-NB-3^{MDR1} cells displayed high fluorescence due to successful transduction with LeGO-vectors (d, f). (C) Flow cytometric analysis of MDR1 expression. (a) Flow cytometric histograms of the cell lines UKF-NB-3 (negative control), UKF-NB-3^{r}VCR^{10} (positive control), UKF-NB-3 transduced with 100 μl of control vector LeGO-Cer2 (UKF-NB-$3^{LeGO\text{-}Cer2}$) and UKF-NB-3 transduced with 100 μl of human MDR1-expressing vector LeGO-iCer2b-MDR1 (UKF-NB-3^{MDR1}). (b) Quantitative analysis of flow cytometry data. *$P < .05$ relative to nontransduced UKF-NB-3 cells. (D) Flow cytometric analysis of MDR1 expression in the cell lines UKF-NB-3, UKF-NB-3^{r}VCR^{10}, UKF-NB-$3^{LeGO\text{-}Cer2}$, and UKF-NB-3^{MDR1} untreated (black bars), treated with 10 μM saquinavir for 5 days (gray bars) or treated with 10 μM saquinavir-NO for 5 days (dark gray bars). Incubation with saquinavir or saquinavir-NO had no influence on MDR1 expression. (E) Concentrations that decrease cell viability by 50% (IC_{50}) for the MDR1 substrate vincristine investigated by MTT assay (values are means ± SD). MDR1-expressing cell lines UKF-NB-3^{MDR1} and UKF-NB-3^{r}VCR^{10} showed higher IC_{50} values for vincristine compared with MDR1-negative cell lines UKF-NB-3 and UKF-NB-$3^{LeGO\text{-}Cer2}$. $^{1}P < .05$ relative to UKF-NB-3. $^{2}P < .05$ relative to UKF-NB-3^{r}VCR^{10}. $^{3}P < .05$ relative to UKF-NB-3^{MDR1}.

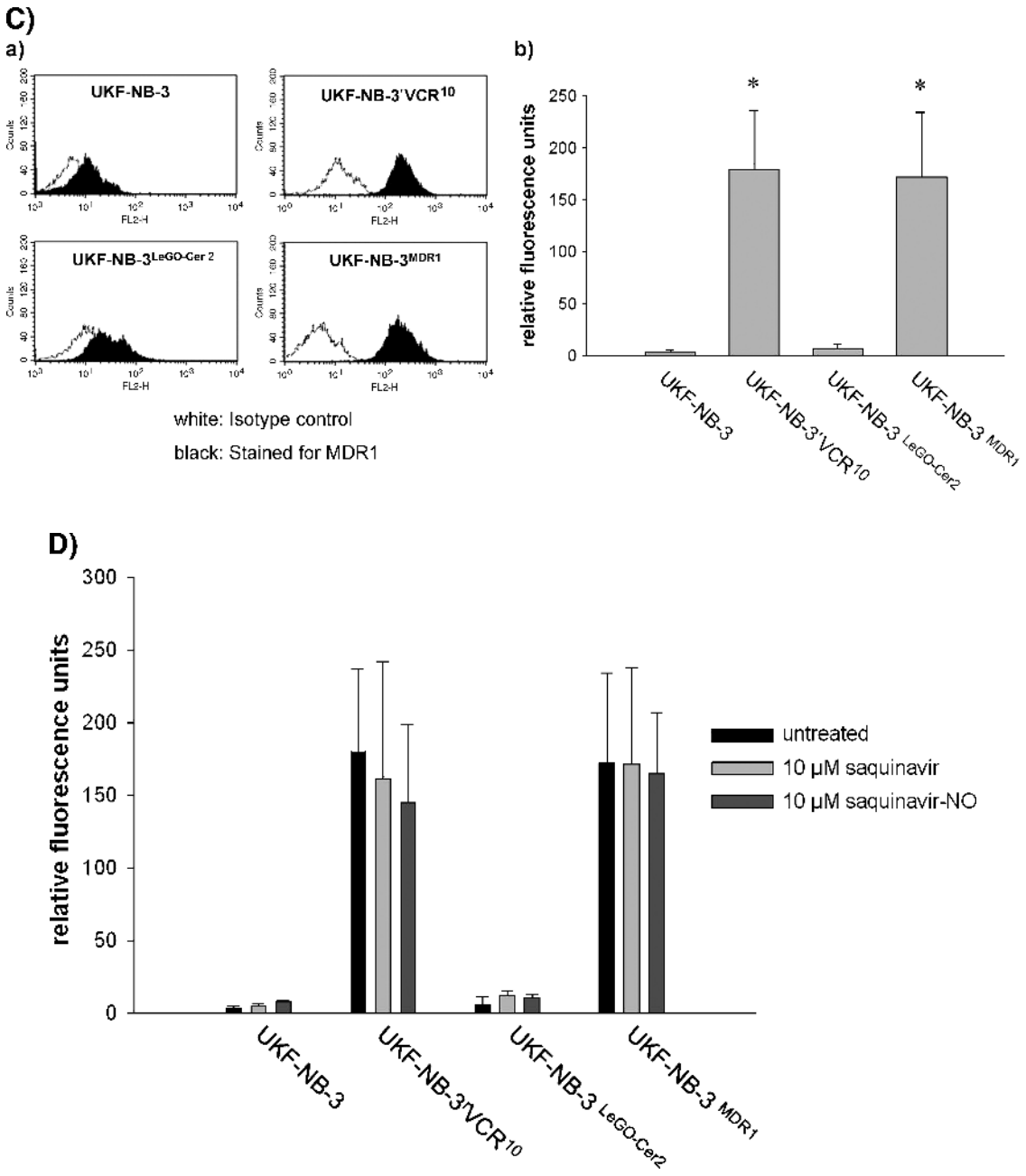

E)

Cell line	IC_{50} vincristine (ng/ml)	IC_{50} vincristine (ng/ml) + verapamil (10µM)
UKF-NB-3	0.20 ± 0.08	0.15 ± 0.07
UKF-NB-3'VCR^{10}	40.29 ± 5.07[1]	1.16 ± 0.21[2]
UKF-NB-3$^{LeGO-Cer2}$	0.28 ± 0.02	0.32 ± 0.09
UKF-NB-3^{MDR1}	13.17 ± 1.35[1]	0.13 ± 0.06[3]

Figure W2. (*continued*).

Materials and Methods

Cloning of Lentiviral Vectors

Standard molecular cloning techniques were used to generate viral vectors based on Lentiviral Gene Ontology (LeGO) vectors [1] (also http://www.LentiGO-Vectors.de). Maps and sequence data of the vectors are available on request. In the first step, the multiple cloning site of the lentiviral vector LeGO-Cer2 was inverted, resulting in LeGO-iCer2b. Then, the 3842-bp cDNA of the human *MDR1* gene was taken out of the γ-retroviral vector SF91m3.IRES.GFP [2,3] (kindly provided by A. Schambach and C. Baum, MH Hannover, Germany) and cloned into LeGO-iCer2b using *Bam*HI and *Not*I. The internal SFFV promoter of this vector transcribes a bicistronic messenger RNA (mRNA) with an internal ribosome entry site (IRES) of the encephalomyocarditis virus (EMCV), expressing the hMDR1 together with the blue fluorescent protein Cerulean as a marker. The vector LeGO-Cer2 only expressing Cerulean served as a control.

Generation of Viral Particles

Cell-free viral supernatants were generated by transient transfection of 293T packaging cells as described [4], using the third-generation packaging plasmids pMDLg/pRRE and pRSV-Rev [5] together with phCMV-VSV-G [4]. Supernatants containing pseudotyped vector particles were titrated on 293T target cells. Gene transfer rates were analyzed 2 days after transduction by fluorescence-activated cell sorting (FACS). Titers of 4×10^6 (LeGO-iCer2b-MDR1) and 8×10^6 (LeGO-Cer2) VSV-G pseudotyped virus particles per milliliter of unconcentrated supernatants were obtained.

Cell Culture and Lentiviral Gene Transfer

All cells were cultured in their respective growth medium supplemented with penicillin/streptomycin. For transduction of UKF-NB-3 target cells, 5×10^4 cells in 500 μl of medium were plated per well in a 24-well plate. The next day, 250 μl of viral supernatant per well was added in the presence of 8 μg/ml polybrene, and the plate was centrifuged at 1000*g* for 1 hour at room temperature. After another 3 hours in the cell culture incubator, medium was replaced.

Fluorescence Microscopy

Pictures were taken using an IX71 fluorescence microscope (Olympus, Hamburg, Germany). Fluorescence dye Cerulean was detected at 433 nm emission/475 nm excitation.

Flow Cytometric Analysis

Flow cytometric data were acquired using the cytometer FACS-Calibur (488 nm laser; Becton Dickinson, Heidelberg, Germany). Staining of hMDR1-positive cells was carried out using an anti–P-glycoprotein antibody (Alexis Biochemicals through AXXORA Deutschland, Lörrach, Germany), followed by staining with a secondary PE-labeled antibody (R&D, Wiesbaden, Germany).

MTT Assay

Cell viability was tested by the 3-(4,5-dimethylthiazol-2-yl)-2,5-diphenyltetrazolium bromide (MTT) dye reduction assay after 96 hours of incubation modified as described before [6].

References

[1] Weber K, Bartsch U, Stocking C, and Fehse B (2008). A multicolor panel of novel lentiviral "gene ontology" (LeGO) vectors for functional gene analysis. *Mol Ther* **16**, 698–706.

[2] Schambach A, Wodrich H, Hildinger M, Bohne J, Kräusslich HG, and Baum C (2000). Context dependence of different modules for posttranscriptional enhancement of gene expression from retroviral vectors. *Mol Ther* **2**, 435–445.

[3] Hildinger M, Schilz A, Eckert HG, Bohn W, Fehse B, Zander A, Ostertag W, and Baum C (1999). Bicistronic retroviral vectors for combining myeloprotection with cell-surface marking. *Gene Ther* **6**, 1222–1230.

[4] Beyer WR, Westphal M, Ostertag W, and von Laer D (2002). Oncoretrovirus and lentivirus vectors pseudotyped with lymphocytic choriomeningitis virus glycoprotein: generation, concentration, and broad host range. *J Virol* **76**, 1488–1495.

[5] Dull T, Zufferey R, Kelly M, et al. (1998). A third-generation lentivirus vector with a conditional packaging system. *J Virol* **72**, 8463–8471.

[6] Michaelis M, Suhan T, Cinatl J, Driever PH, and Cinatl J, Jr (2004). Valproic acid and interferon-alpha synergistically inhibit neuroblastoma cell growth *in vitro* and *in vivo*. *Int J Oncol* **25**, 1795–1799.

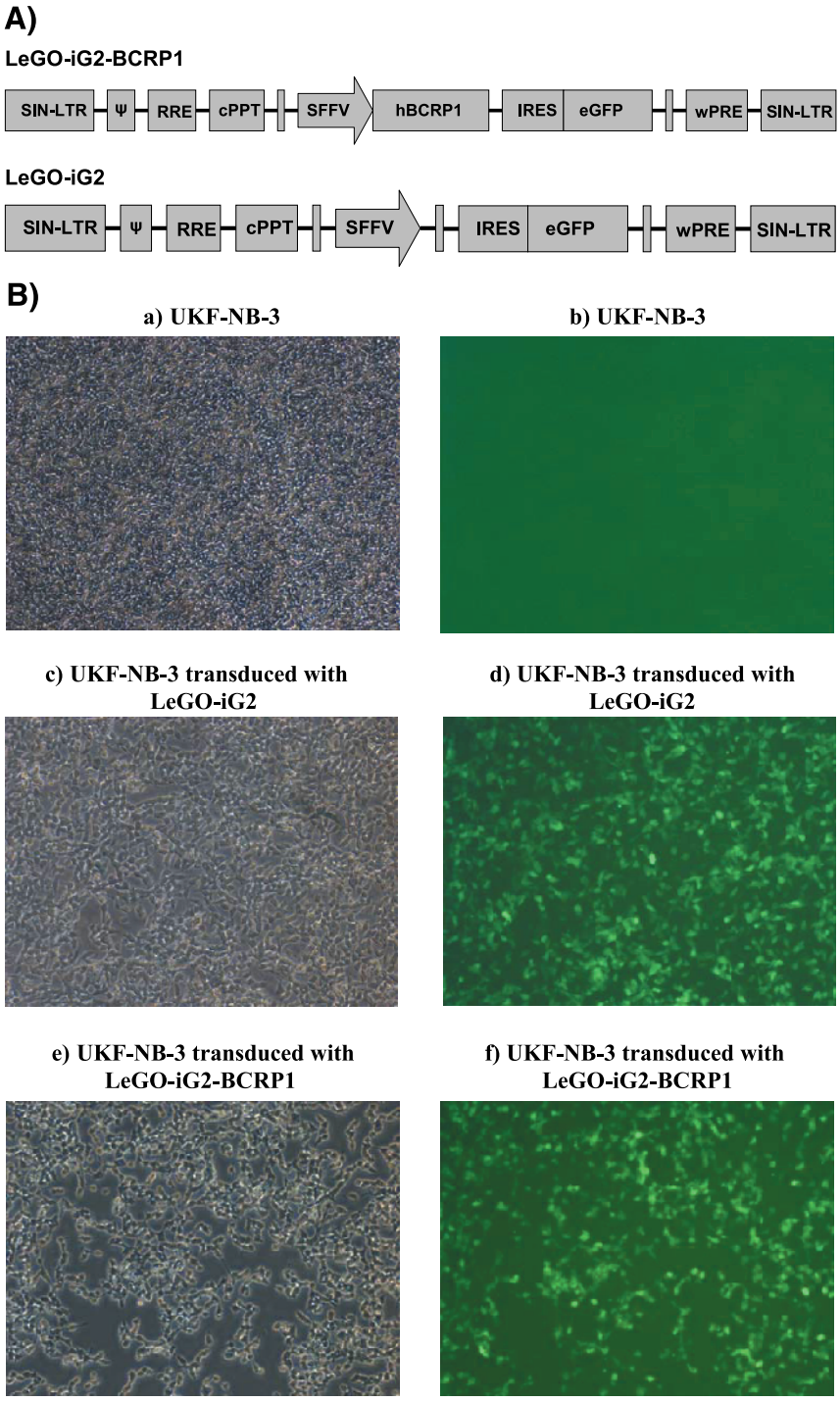

Figure W3. (A) Scheme of the lentiviral vectors, as integrated proviruses, that have been used in this study (not drawn to scale). Ψ indicates packaging signal; cPPT, central polypurine tract; eGFP, enhanced green fluorescent protein; hBCRP1, human breast cancer resistance protein 1 gene cDNA; IRES, internal ribosome entry site of the EMCV; RRE, rev-responsive element; SFFV, spleen focus–forming virus enhancer/promoter; SIN-LTR, self-inactivating long terminal repeat; wPRE, Woodchuck hepatitis virus posttranscriptional regulatory element. (B) UKF-NB-3 cells, UKF-NB-3 cells transduced with LeGO-iG2 (UKF-NB-3$^{LeGO\text{-}iG2}$), and UKF-NB-3 cells transduced with LeGO-iG2-BCRP1 (UKF-NB-3^{BCRP1}) were photographed by inverse light microscopy (a, c, e) and by fluorescence microscopy (b, d, f) using an IX71 fluorescence microscope (Olympus). Fluorescence dye eGFP was detected at 484/507 nm (excitation/emission). The nontransduced control cell line UKF-NB-3 showed no fluorescence (b). In contrast, UKF-NB-3$^{LeGO\text{-}iG2}$ and UKF-NB-3^{BCRP1} cells displayed high fluorescence due to successful transduction with LeGO vectors (d, f). (C) Flow cytometric analysis of BCRP1 expression. (a) Flow cytometric histograms of the cell lines UKF-NB-3 (negative control), UKF-NB-3 transduced with 100 μl of control vector LeGO-iG2 (UKF-NB-3$^{LeGO\text{-}iG2}$) and UKF-NB-3 transduced with 100 μl of human BCRP1-expressing vector LeGO-iG2-BCRP1 (UKF-NB-3^{BCRP1}). (b) Quantitative analysis of flow cytometry data. *$P < .05$ relative to nontransduced UKF-NB-3 cells. (D) Flow cytometric analysis of BCRP1 expression in the cell lines UKF-NB-3, UKF-NB-3$^{LeGO\text{-}iG2}$, and UKF-NB-3^{BCRP1} untreated (black bars), treated with 10 μM saquinavir for 5 days (gray bars) or treated with 10 μM saq-NO for 5 days (dark gray bars). Incubation with saquinavir or saquinavir-NO had no influence on BCRP1 expression. (E) Concentrations that decrease cell viability by 50% (IC_{50}) for the BCRP1 substrate mitoxantrone, determined by MTT assay (values are means ± SD) in the absence or presence of the BCRP1 inhibitor WK-X-34. BCRP1-expressing cell line UKF-NB-3^{BCRP1} showed higher IC_{50}-values for mitoxantrone compared with BCRP1-negative cell lines UKF-NB-3 and UKF-NB-3$^{LeGO\text{-}iG2}$. [1]$P < .05$ relative to UKF-NB-3. [2]$P < .05$ relative to UKF-NB-3^{BCRP1}.

C)

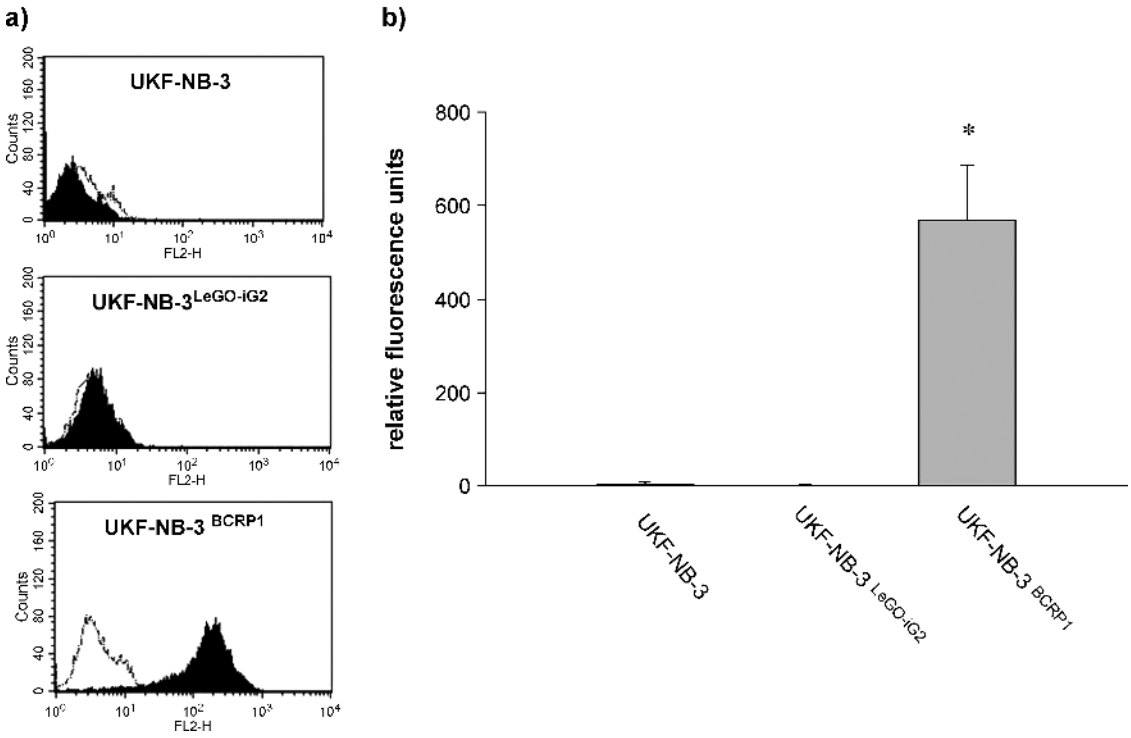

D)

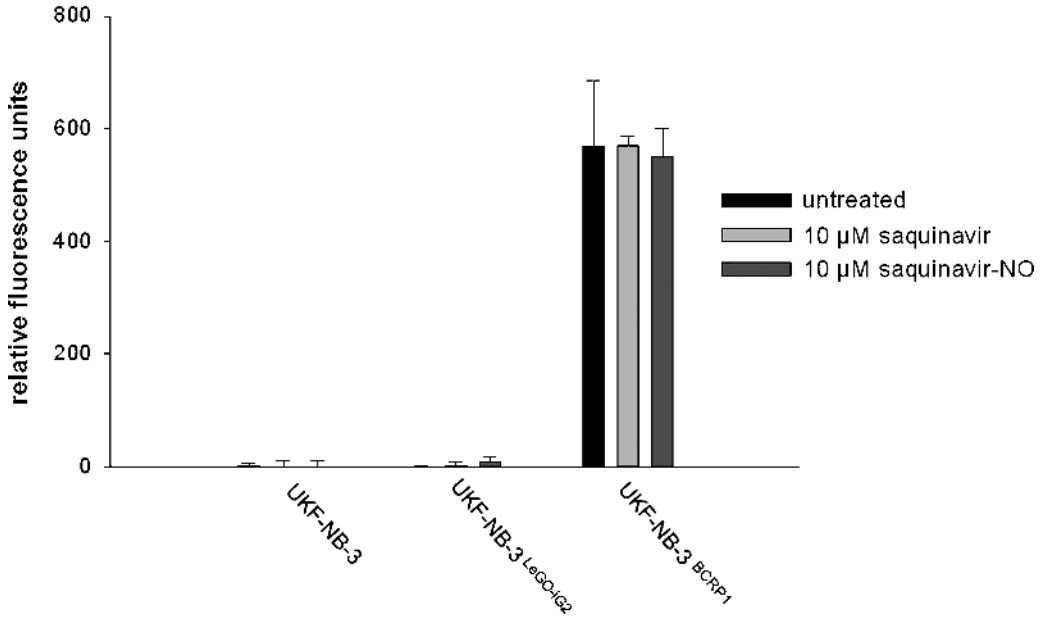

E)

Cell line	IC_{50} mitoxantrone (ng/ml)	IC_{50} mitoxantrone (ng/ml) + WK-X-34 (1µM)
UKF-NB-3	0.18 ± 0,084	0.16 ± 0.039
UKF-NB-3$^{LeGO-iG2}$	0.21 ± 0,056	0.23 ± 0.061
UKF-NB-3^{BCRP1}	45.87 ± 7,97[1]	0.17 ± 0.042[2]

Figure W3. (*continued*).

Materials and Methods of Viral Transduction

Cloning of Lentiviral Vectors

Standard molecular cloning techniques were used to generate viral vectors based on Lentiviral Gene Ontology (LeGO) vectors [1] (also http://www.LentiGO-Vectors.de). Maps and sequence data of the vectors are available on request. The lentiviral vector LeGO-iG2 was used as backbone vector. Then, the 1968-bp cDNA of the human *BCRP1* gene was cloned into LeGO-iG2 using *Bam*HI and *Not*I. The internal SFFV promoter of this vector transcribes a bicistronic mRNA with an IRES of the EMCV, expressing the hBCRP1 together with the enhanced green fluorescent protein (eGFP) as a marker. The vector LeGO-iG2 only expressing GFP served as a control.

Generation of Viral Particles

Cell-free viral supernatants were generated by transient transfection of 293T packaging cells as described [2], using the third-generation packaging plasmids pMDLg/pRRE and pRSV-Rev [3] together with phCMV-VSV-G [2]. Supernatants containing pseudotyped vector particles were titrated on 293T target cells. Gene transfer rates were analyzed 2 days after transduction by fluorescence-activated cell sorting (FACS). Titers of 2.4×10^6 (LeGO-iG2-BCRP1) and 5×10^6 (LeGO-iG2) VSV-G pseudotyped virus particles per milliliter of unconcentrated supernatants were obtained.

Cell Culture and Lentiviral Gene Transfer

All cells were cultured in their respective growth medium supplemented with penicillin/streptomycin. For transduction of UKF-NB-3 target cells, 5×10^4 cells in 500 µl of medium were plated per well in a 24-well plate. The next day, 250 µl of viral supernatant per well was added in the presence of 8 µg/ml polybrene, and the plate was centrifuged at 1000*g* for 1 hour at room temperature. After another 3 hours in the cell culture incubator, medium was replaced.

Fluorescence Microscopy

Pictures were taken using an IX71 fluorescence microscope (Olympus, Hamburg, Germany). Fluorescence dye eGFP was detected at 484 nm emission/507 nm excitation.

FACS Analysis

FACS data were acquired using the cytometer FACSCalibur (488 nm laser; Becton Dickinson, Heidelberg, Germany). Staining of hBCRP1-positive cells was carried out using an anti-hBCRP1 antibody (Kamiya Biomedical Company, Seattle, WA) followed by staining with a secondary PE-labeled antibody (R&D, Wiesbaden, Germany).

MTT Assay

Cell viability was tested by the 3-(4,5-dimethylthiazol-2-yl)-2,5-diphenyltetrazolium bromide (MTT) dye reduction assay after 96 hours of incubation modified as described before [4].

References

[1] Weber K, Bartsch U, Stocking C, and Fehse B (2008). A multicolor panel of novel lentiviral "gene ontology" (LeGO) vectors for functional gene analysis. *Mol Ther* **16**, 698–706.

[2] Beyer WR, Westphal M, Ostertag W, and von Laer D (2002). Oncoretrovirus and lentivirus vectors pseudotyped with lymphocytic choriomeningitis virus glycoprotein: generation, concentration, and broad host range. *J Virol* **76**, 1488–1495.

[3] Dull T, Zufferey R, Kelly M, Mandel RJ, Nguyen M, Trono D, and Naldini L (1998). A third-generation lentivirus vector with a conditional packaging system. *J Virol* **72**, 8463–8471.

[4] Michaelis M, Suhan T, Cinatl J, Driever PH, and Cinatl J, Jr (2004). Valproic acid and interferon-alpha synergistically inhibit neuroblastoma cell growth *in vitro* and *in vivo*. *Int J Oncol* **25**, 1795–1799.